

Distribution Agreement

In presenting this thesis as a partial fulfillment of the requirements for a degree from Emory University, I hereby grant to Emory University and its agents the non-exclusive license to archive, make accessible, and display my thesis in whole or in part in all forms of media, now or hereafter now, including display on the World Wide Web. I understand that I may select some access restrictions as part of the online submission of this thesis. I retain all ownership rights to the copyright of the thesis. I also retain the right to use in future works (such as articles or books) all or part of this thesis.

Johanna Ben-Ami

March 16, 2016

Smo^{AW4}: A novel hypomorphic allele

by

Johanna Ben-Ami

Dr. Tamara Caspary
Adviser

Department of Biology

Dr. Tamara Caspary
Adviser

Dr. Victor Corces
Committee Member

Dr. Levi Morran
Committee Member

2016

Smo^{AW4}: A novel hypomorphic allele

By

Johanna Ben-Ami

Dr. Tamara Caspary
Adviser

An abstract of
a thesis submitted to the Faculty of Emory College of Arts and Sciences
of Emory University in partial fulfillment
of the requirements of the degree of
Bachelor of Sciences with Honors

Department of Biology

2016

Abstract

Smo^{AW4}: A novel hypomorphic allele

By Johanna Ben-Ami

Vertebrate hedgehog signaling is essential for patterning and cell proliferation during development. Overactivation of the Sonic Hedgehog (Shh) signaling pathway is the cause of some cancers, and both increased and decreased signaling can cause intellectual disability. Within this pathway Smoothed (Smo) is the obligate transducer, thus necessary for activation of downstream signal targets. We have isolated a novel mutant, *Smo^{AW4}*, which survives longer than the null allele. Our mutant is able to survive until birth, but dies thereafter. We identified an asparagine to lysine change at residue 223 in *Smo^{AW4}*, which I hypothesize acts as a hypomorphic allele. The mutant presents with craniofacial, limb, and neural tube abnormalities, consistent with Smo's importance in Shh signaling transduction. During development, protein expression is essential in patterning the neural tube, which becomes the organism's future spinal cord. Shh signaling plays a vital role in specification of progenitor cells via Smo. I analyzed neural patterning using fluorescent antibody staining at e9.5, e10.5, and e11.5. I found the patterning to be abnormal, with ventral expansion of the motor neuron progenitors indicating lower Shh activity, consistent with *Smo^{AW4}* being a hypomorphic allele. Next, I examined fibroblasts derived from the mutants by quantitative RT-PCR looking at downstream pathway targets *Gli1* and *Patched1*, which I hypothesized would be reduced from the wild type but still present. I found *Patched1* RNA expression to be significantly reduced in the mutants when Shh treated, and *Gli1* RNA expression was also reduced, with a strong trend toward significance. Primary cilia are involved in detecting sensory information for the cell, and are where Shh signaling occurs. Although there are clear links between primary cilia and Shh signaling, the mechanism is not fully understood. During vertebrate Shh signaling, Smo is enriched within the cilium. I looked for enrichment of Smo within the cilium, and preliminary results suggest that the mutant allele does not have this enrichment when Shh treated. Taken together, the results indicate that *Smo^{AW4}* is a hypomorphic allele and suggest that ciliary enrichment is not absolutely required for pathway activation.

Smo^{AW4}: A novel hypomorphic allele

By

Johanna Ben-Ami

Dr. Tamara Caspary
Adviser

A thesis submitted to the Faculty of Emory College of Arts and Sciences
of Emory University in partial fulfillment
of the requirements of the degree of
Bachelor of Sciences with Honors

Department of Biology

2016

Acknowledgements

I would like to thank Alyssa Long and Tamara Caspary for their mentorship and support throughout my time in the lab. I would also like to thank Sarah Bay and Laura Mariani for their help with statistical analyses and cell culture. In addition, thank you to the entirety of the Caspary Lab, Tim Rutkowski, Sarah Suci, and Chao Lin, for your continuous support and encouragement.

Several of the monoclonal antibodies used in this work were obtained from the Developmental Studies Hybridoma Bank, created by the NICHD of the NIH and maintained at The University of Iowa, Department of Biology, Iowa City, IA 52242.

Table of Contents

| | |
|--|----|
| Introduction | 1 |
| Materials and Methods | 6 |
| Mouse Information | 6 |
| Immortalization of MEFs | 6 |
| Cell Culture | 7 |
| Immunofluorescent Antibody Staining | 8 |
| Quantitative Reverse Transcription-PCR | 10 |
| Statistical Analysis | 11 |
| Results | 11 |
| Discussion | 16 |
| References | 20 |

List of Figures:

| | |
|---|----|
| Figure 1: Diagram of the Sonic Hedgehog signaling pathway | 2 |
| Figure 2: Alignment of protein sequences from select species | 4 |
| Figure 3: Schematic diagram of the Smoothened protein | 4 |
| Figure 4: Frontal view of <i>Smo^{AW4}</i> mutant embryo | 5 |
| Figure 5: Side view of <i>Smo^{AW4}</i> mutant embryo | 5 |
| Figure 6: View of <i>Smo^{AW4}</i> limb abnormalities | 6 |
| Figure 7: Schematic of normal neural patterning | 11 |
| Figure 8: Wild type neural tube immunofluorescence staining | 12 |
| Figure 9: <i>Smo^{AW4}</i> neural tube immunofluorescence staining | 12 |
| Figure 10: <i>Gli1</i> transcriptional response to Shh stimulation in <i>Smo^{AW4}</i> MEFs | 13 |
| Figure 11: <i>Patched1</i> transcriptional response to Shh stimulation in <i>Smo^{AW4}</i> MEFs | 13 |
| Figure 12: Wild type Shh-treated cell stained for acetylated alpha tubulin and Smo | 14 |
| Figure 13: <i>Smo^{AW4}</i> Shh-treated cell stained for acetylated alpha tubulin and Smo | 14 |
| Figure 14: Graph showing percentage of cells with cilia and Smo | 15 |
| Figure 15: <i>Gli1</i> transcriptional response to SAG stimulation | 15 |
| Figure 16: <i>Patched1</i> transcriptional response to SAG stimulation | 16 |
| Figure 17: Binding pocket for antitumor agent LY2940680, in human Smoothened | 19 |

Introduction:

Vertebrate Hedgehog signaling is a critical regulator of patterning and cell proliferation during embryonic development (1). There are three vertebrate Hh ligands: Sonic Hedgehog (Shh), Indian Hedgehog (Ihh) and Desert Hedgehog (Dhh). Underactivation of Sonic Hedgehog affects the tissue developmental patterning function of Shh signaling (2). Over activation of Shh signaling can cause excess proliferation and tumorigenesis, thus resulting in a plethora of cancers, including basal cell carcinoma and medulloblastoma. Both increased and decreased Shh signaling results in limb and craniofacial defects, and underactivation is thought to cause intellectual disability. The clinical importance of Shh signaling has led to a need to understand the pathway's regulation in order to develop therapeutics that would re-regulate abnormal signaling back to the normal, balanced level. Although the scientific community has learned a lot about Shh signaling, there is still a great deal that we do not know.

In addition to the three ligands, at the core of vertebrate Hh signaling are Patched1 (Ptch), Smoothed (Smo), and three Gli proteins, Gli1, Gli2 and Gli3 (Figure 1). In the absence of Shh, Ptch inhibits Smo; this interaction is not direct but is understood to be inhibitory because when Ptch is absent, signaling is constitutive (3). During signaling, Shh binds its receptor, Ptch, allowing Smo to activate downstream targets of the pathway (4). Smo activates the three Gli proteins, which then promote expression of target genes. Smo is the obligate transducer for all vertebrate Hedgehog signaling (5-7). In vertebrates, enrichment of Smo into primary cilia is central to pathway activation. Although Smo is evolutionarily conserved in both fly and vertebrates, the use of cilia is vertebrate specific (8). Different cellular responses to Shh signaling occur in different tissues due to regulation

of tissue specific target genes (1). In addition to these core components of the pathway, there are many other proteins that regulate each step, yet we do not understand all of the intricate details, so many questions remain to be answered.

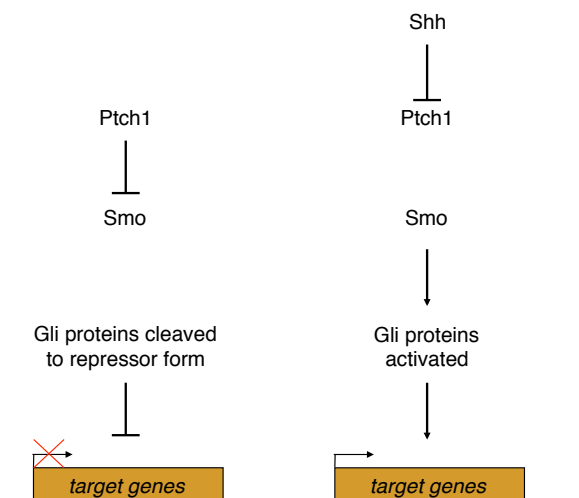


Figure 1: Diagram of the Sonic Hedgehog signaling pathway. Left: no Sonic ligand Right: presence of Sonic ligand

Shh plays an important role in patterning embryonic tissues including the neural tube, the axial skeleton, the face and limbs. Indeed, Shh null mouse models display an absence of distal limb structures, cyclopia, and holoprosencephaly (2). Additionally, Shh signaling plays an integral role in specification of cell fates along the dorsal-ventral axis of the neural tube, a process called dorso-ventral patterning (2). Chiang and colleagues found no ventral cell fate specification in the neural tubes of Shh null mutants indicating Shh is essential to the process (2). Subsequently, distinct concentrations of Shh elicited the different cell fates in neural tube culture (2). Together these data lead to the proposal that Shh acts as a long-range morphogen that controls cell patterning and differentiation in the vertebrate neural tube (9-11).

Progenitor cells of the spinal cord differentiate into their specific fates based on the combination of transcription factors they express. Shh is produced in the notochord,

underlying the ventral midline of the neural tube, and subsequently in the floor plate, at the ventral midline of the neural tube. Transcription factors such as Olig2, Nkx2.2, FoxA2, and HB9 are induced at discrete distances from the notochord by distinct Shh activity levels, resulting in the patterning of the neural tube. FoxA2 is expressed in the floor plate. Adjacent to the floor plate is the p3 region expressing Nkx2.2. Dorsal to the p3 region are the pMN cells that express Olig2. Olig2 positive cells differentiate to motor neurons, which express HB9 and migrate outwards or laterally. Thus changes to neural patterning cause significant defects in the development of the central nervous system.

Null alleles of Smo have allowed the scientific community to learn a lot about vertebrate Hedgehog signaling and the role of Smo within the pathway (12, 13). Smo null mutants do not survive past embryonic day 9.5 (e9.5), and exhibit ventral cyclopia and holoprosencephaly similar to Shh mutants, consistent with Smo being essential to transmit Shh signal. However, Smo mutants were more severely affected than Shh mutants, which survive almost to birth. This more severe phenotype illustrates that Smo also transduces Ihh and Dhh signaling in addition to Shh (13). Although such information has been fruitful in increasing our understanding of this pathway, humans cannot survive with completely depleted Hh signaling. A hypomorphic mutation in Smo would serve as an additional model to better understand the mechanistic details of the pathway and etiology of human disease.

Prior to my involvement in Dr. Caspary's lab, her lab performed an ENU-induced forward genetic screen where they found 17 novel mutations that disrupted neural development. Through genetic mapping and deep resequencing they identified the mutations responsible for the phenotypes (14). I chose to study one line carrying a novel allele of *Smo*, called AW4. *Smo*^{AW4} is an asparagine to lysine change at residue 223, an

evolutionarily conserved residue (Figure 2). Smo is a G-protein coupled receptor with seven transmembrane domains (15). The mutation lies right outside the cell membrane just prior to the first transmembrane domain (Figure 3). The structure of Smo shows that this residue lies in a pocket that has been targeted by drugs that inhibit Smo activity (15,16). This supports the importance and functionality of this residue.

Smo^{AW4} N223K

| | | |
|-----------|-----|--|
| Human | 151 | DRFPEGCTNEVQNIKFNSSGQCEVPLVVRTDNPKSWYEDVEGCGIQCQ NP |
| Mouse | 176 | DHFPEGCPNEVQNIKFNSSGQCEAPLVVRTDNPKSWYEDVEGCGIQCQ NP |
| Chicken | 72 | DRFPEGCPNEVQNIKFNSSGQCEAPLVVRTDNPKSWYEDVEGCGIQCQ NP |
| Zebrafish | 151 | EQFPKGCQNEVQKLFNTSGQCEAPLVKTDIQASWYKDVEGCGIQCD NP |

Figure 2: Alignment of protein sequences from select species. Illustrates evolutionary conservation of the N residue

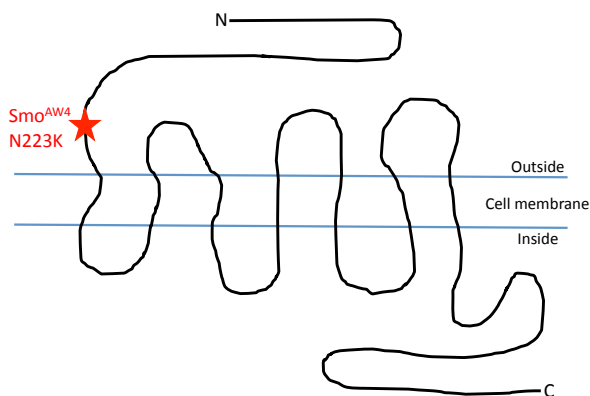


Figure 3: Schematic diagram of Smoothened protein showing transmembrane domains and location of the AW4 mutation

The *Smo*^{AW4} mutants survive until birth, but not thereafter. The phenotype is consistent with the importance of Smo in the transduction of Shh signaling. Craniofacially, the nasal pits on these mutant embryos are both more medial and vertical at e10.5 as compared to the wild type whose nasal pits are more diagonal and lateral (Figure 4). At e10.5 through e12.5, the dorsal part of the neural tube appears rough and bumpy when compared to the smooth dorsal neural tube of the wild type (Figure 5). At e12.5 the *Smo*^{AW4}

mutant presents with shortened digits and limbs, consistent with the role of Shh signaling in limb development (Figure 6). The rough and bumpy neural tube phenotype was what led us to analyze neural patterning. Since this mutation is within Smo but causes a less severe phenotype when compared to complete nulls, I hypothesize that *Smo*^{AW4} is a hypomorphic allele that can be used to better understand the Shh signaling pathway.



Figure 4: Frontal view of e10.5 wild type and *Smo*^{AW4} mutant embryos showing craniofacial defects

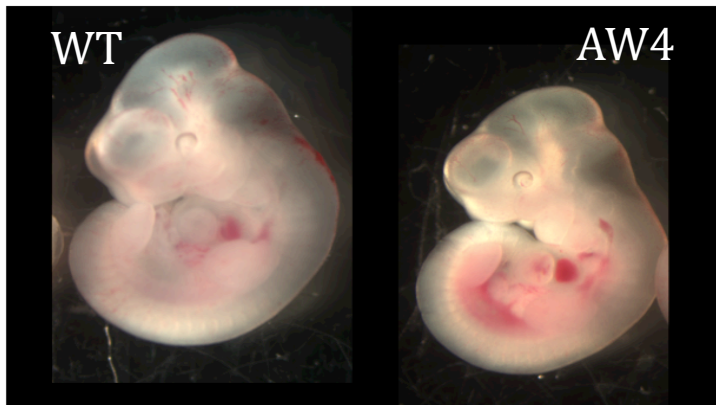


Figure 5: Side view of e10.5 wild type and *Smo*^{AW4} mutant embryos showing dorsal neural tube abnormalities

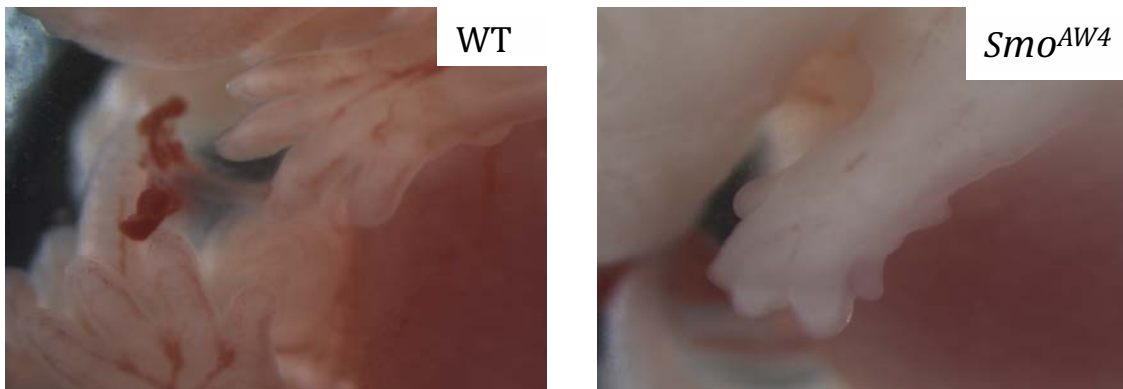


Figure 6: Side view of e10.5 wild type and *Smo^{AW4}* mutant embryos showing limb abnormalities

Materials and Methods:

Mouse information:

Prior to my involvement in Dr. Tamara Caspary's lab, Sun and colleagues performed a recessive ENU mutagenesis screen as previously described (14). C57BL/6J mice were mutagenized and crossed to FVB/NJ. Female offspring were backcrossed to F1 males to homozygose the mutation for morphological examination in embryos. G3 embryos were examined at e10.5 for abnormal nervous system development. By using a genome scan utilizing single nucleotide polymorphism (SNP) or simple sequence length polymorphism (SSLP) markers, *Smo^{AW4}* was mapped to chromosome 6 (14). For the embryo studies described in this thesis, heterozygous mice were crossed and the female was dissected 10.5 days after copulation, as identified by the presence of a vaginal plug.

Immortalization of MEFs:

Fibroblasts were isolated from e12.5 mutant and wild type embryos. These mouse embryonic fibroblasts (MEFs) were transfected with a construct containing the oncogene SV40 T antigen, which facilitates the cells ability to override cell cycle checkpoints. Next

cells underwent a series of serial dilutions that isolate successfully transformed cells. This series began with a 1:4 dilution and a 1:10 dilution of transfected cells. These two dilution values were chosen to ensure that there were viable cells after the initial dilution. Each dilution was performed by aspirating off the media followed by washing with 5 mL of DPBS (1x Dubecco's Phosphate Buffered Saline with Calcium and Magnesium, Corning Cellgro). Next, the DPBS wash was aspirated off of the plate and 2 mL of Trypsin (0.25% Trypsin, 2.21 mM EDTA, Corning Cellgro) was added to the cells in order to remove the cells from the plate. Trypsinized cells were placed in an incubator at 37 degrees for 2 minutes. Next, 8 mL of media was added to the cells, ensuring that as many cells as possible were released from the plate. Depending on the dilution factor, either 2.5 mL of the original plate was added to 7.5 mL of media in a new plate (for the 1:4 dilution series) or 1 mL of the original plate was added to 9 mL of media in a new plate (for the 1:10 dilution series). MEFs are considered immortalized if they make it to a 1:1,000,000 dilution from the original cell transformation step.

After successful immortalization, cells were split as previously described but in a 1:20 dilution factor, thus 0.5 mL of the trypsinized cells and media solution was added to 9.5 mL of media.

Cell Culture:

Wild type or mutant cells were plated onto a 6-well plate, using only 4-wells per plate. There were 2 wells for immunofluorescence (IF), and 2 wells for quantitative real time-PCR (qPCR). For each Shh treatment experiment, 1-well was given 0.5% FBS in DMEM and 1-well was given sonic hedgehog conditioned media. Similarly, for the SAG IF and qPCR experiments, 1-well was given 0.5% Fetal Bovine Serum (FBS) in Dulbecco's Modification

of Eagle's Medium (DMEM) and 1-well was given SAG conditioned media. Two coverslips were placed into the immunofluorescent protocol wells, and 0.1×10^6 cells were plated in 2 mL of media (Dulbecco's Modification of Eagle's Medium with 4.5 g/L glucose, L-glutamine and sodium pyruvate, Corning Cellgro). 0.3×10^6 cells were plated in 2 mL of media for the qPCR protocol. SAG containing media was made by diluting 10mM stock SAG 1:20 in DMEM and using 1 μ l of the diluted solution in 5 mL of 0.5% FBS in DMEM. Cells were treated with SAG conditioned media or FBS for 24 hours. After treatment, the cells for immunofluorescence were washed with PBS, fixed in 4% paraformaldehyde for 10 minutes, and then washed with PBS. The qPCR protocol cells were released from the surface of the well using 0.5 mL of trypsin and 1 mL of media and collected in a 1.5 mL conical tube. The cells were then pelleted in a 5-minute spin at 3400 rpm. Media was aspirated off, leaving the cell pellet untouched. Cell pellets were frozen at -80 degrees until use.

Immunofluorescent Antibody Staining:

Embryos were fixed for one hour at 4°C in 4% paraformaldehyde in phosphate buffered saline (PBS). Fix was removed by washing embryos 3 X 40 minutes in PBS at room temperature. Embryos were placed in 30% sucrose, 0.1 M phosphate buffer overnight at 4°C. Embryos were washed 3 X 20 minutes in OCT and then embedded in OCT in the axial position, frozen on dry ice, and stored at -20°C. Embedded embryos were sectioned on the cryostat in 10-micron sections.

Slides were washed in antibody wash solution (1% heat-inactivated goat serum, 0.1% Triton X-100 in PBS) for 10 minutes. Primary antibodies were diluted in antibody wash solution as follows: mouse anti-Shh, mouse anti-FoxA2, mouse anti-HB9, mouse anti-

Nkx2.2 each at 1:5 (Developmental Studies Hybridoma Bank), or rabbit anti-Olig2 at 1:200 (Millipore). 150 μ l of diluted primary antibody solution was pipetted on each slide, covered with parafilm and incubated in a flat humidified chamber overnight at 4°C.

Coverslips were also washed in antibody wash solution for 10 minutes. Primary antibodies were diluted in antibody wash solution as follows: mouse anti-acetylated alpha tubulin at 1:2500 (Sigma Aldrich), rabbit anti-Smoothed at 1:500 (gift from Kathryn Anderson), and rabbit anti-Arl13b at 1:1500 (made by Dr. Caspary in the Anderson Lab) (16). 60 μ l of diluted primary antibody solution was pipetted on each coverslip, covered and incubated overnight at 4°C.

After overnight incubation, slides and coverslips were washed 3 X 20 minutes at room temperature with the antibody wash solution. Secondary antibody dilutions were prepared in wash solution as follows: goat anti-mouse Alexafluor 568 or donkey anti-rabbit Alexafluor 568 (each at 1:200, ThermoFisher Scientific). Hoechst stain was used at a 1:300 dilution in wash solution to visualize nuclei. 150 μ l of secondary stain solution was added to each slide in a humidified chamber protected from light and left for 1 hour at room temperature. 60 μ l of secondary stain solution was added to each coverslip and light protected for 1 hour at room temperature. Slides and coverslips were washed 2 X 30 minutes at room temperature in antibody wash solution. Slides were mounted with ProLong Gold antifade reagent (Life Technologies) and examined with a Leica DM6000B microscope within 2-3 days of staining. Five images were taken of each coverslip to ensure a representative sample. Cells were counted using the Fiji image analysis software, and images of the same condition and cell type were averaged for analysis.

Quantitative RT-PCR:

Cell pellets were kept at -80°C until RNA extraction. Cell pellets were lysed with RLT lysis buffer and QIAshredder homogenizer columns (Qiagen). RNA was extracted from cell pellets using the RNeasy kit (Qiagen). cDNA was synthesized using iScript Reverse Transcription Supermix (Bio-Rad) using 200 ng of RNA per reaction. Stock primers were made at 50 mM in 1X TE and diluted 1:100 in water before use. Primers used were:

Ptch1 5'-TGCTGTGCCTGTGGTCATCCTGATT-3', and 5'-CAGAGCGAGCATAGCCCTGTGGTTC-3'; *Gli1* 5'-CTTCACCCTGCCATGAAACT-3', and 5'-TCCAGCTGAGTGTGTCCAG-3'; *Pold3* 5'-ACGCTTGACAGGAGGGGGCT-3', and 5'-AGGAGAAAAGCAGGGGCAAGCG-3'.

Samples were run in technical triplicate. Each reaction contained 2 µL of diluted cDNA, 10 µL Sso Advanced Universal SYBR Supermix (Bio-Rad), 3 µL 1:100 forward primer, 3 µL 1:100 reverse primer, and 2 µL water. A standard curve of a 1:5 dilution series of cDNA from Shh-treated SmoA1-GFP MEFs (generated by Sarah Bay; chosen because these cells express very high levels of Shh target genes and thus can be diluted to capture a large dynamic range of transcript levels) was run on each plate.

Each plate was run on a Bio-Rad CFX96 Touch Real Time PCR Detection System, and data was collected and analyzed using Bio-Rad CFX Manager 3.1 software. The program conditions were: 95°C for 5 min; 45 cycles of 95°C for 15 seconds, 57°C for 30 seconds, plate read; and generation of a melt curve beginning at 65°C and ending at 95°C.

Starting quantities (in arbitrary units) were determined from comparison to the standard curve. Each triplicate set of technical replicates was averaged to give a value for a single biological replicate. *Gli1* and *Ptch1* expression levels were then normalized to the corresponding *Pold3* levels for each replicate of a given sample.

Statistical Analysis:

Quantitative RT-PCR results were analyzed using a two-way ANOVA with multiple tests using the Prism statistical software package. Results were corrected for multiple tests using a Bonferroni correction, yielding a threshold p-value of 0.0125.

Results:

Neural Patterning Phenotype:

If *Smo^{AW4}* functions as a hypomorphic allele, I would expect decreased, but not absent, Shh activity. As neural patterning is exquisitely sensitive to Shh activity levels, I investigated whether ventral cell fates were disrupted in *Smo^{AW4}* by examining Shh, FoxA2, Nkx2.2, Olig2, and HB9 expression using immunofluorescent antibody staining. As mentioned in the introduction, the expression of these proteins define specific subpopulations of cells (9). Shh positive cells reside in the notochord and the floor plate, FoxA2 positive cells are found in the floor plate, Nkx2.2 positive cells are located in p3, Olig2 positive cells are located in pMN and HB9 positive cells are lateral to the Olig2 positive cells (Figure 7) (10).

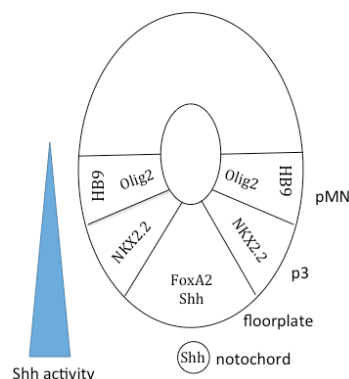


Figure 7: Diagram of proteins examined by IF staining, showing normal expression in a wild type e10.5 neural tube

In the *Smo^{AW4}* mutant embryos, I found the cell fates were correctly specified but their location was shifted towards the ventral midline. Additionally, the domains appeared smaller relative to the wild type (Figures 8 and 9). These data suggest that *Smo^{AW4}* mutants possess less Shh activity in the neural tube, consistent with my hypothesis that *Smo^{AW4}* is a hypomorphic allele.

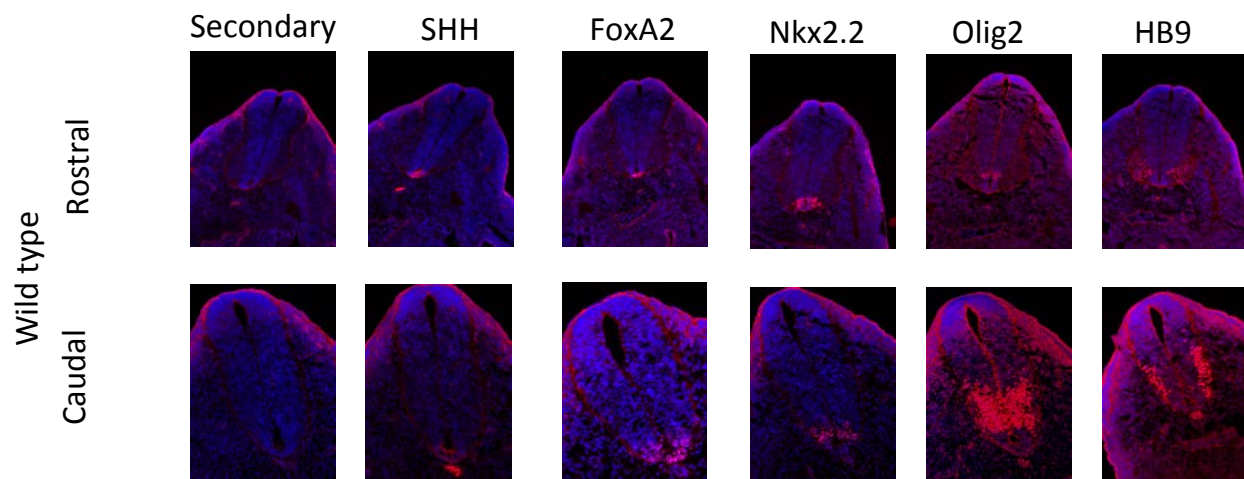


Figure 8: Wild type neural tube patterning, the ventral cell fates expressing specific transcription factors. Neural development occurs in a rostral to caudal gradient, so the rostral neural tube is further developed than the caudal neural tube.

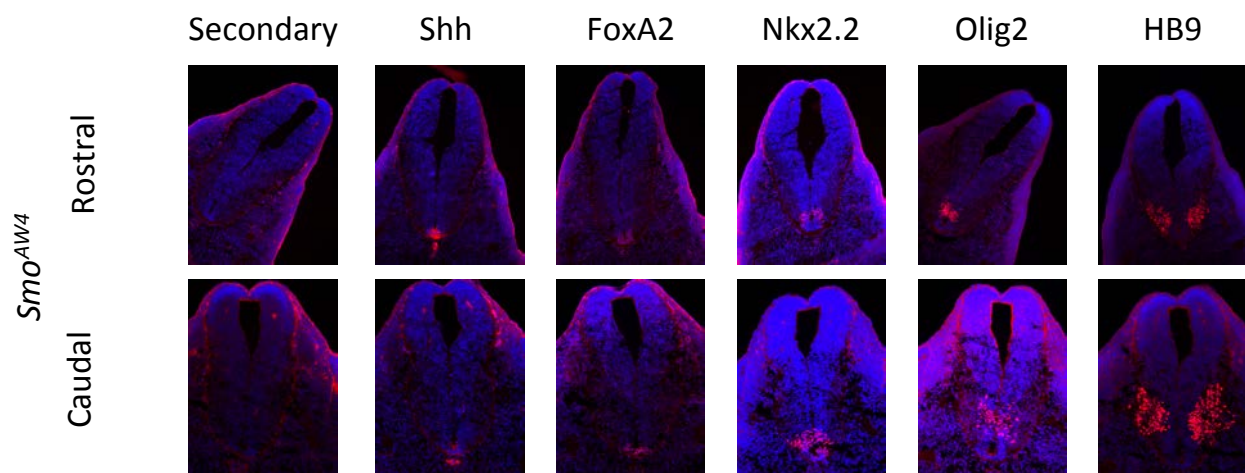


Figure 9: The patterning exhibited by *Smo^{AW4}* illustrates reduced domains of Shh-dependent cell fates. These data are consistent with *Smo^{AW4}* being a hypomorphic allele of Smoothed, in congruence with the change of an evolutionary conserved amino acid.

Quantitative RT-PCR:

I used qPCR to measure the presence of Shh transcriptional targets, *Gli1* and *Patched1*. My *Gli1* results are trending towards statistically significant, consistent with decreased but still present transduction of the pathway (Figure 10). The Bonferroni correction for four tests yields a p-value $< .0125$, and the comparison between wild type and *Smo^{AW4}* *Gli1* after Sonic Hedgehog treatment yields a p-value of .0134. This indicates that *Gli1* expression is strongly trending towards statistical significance, consistent with my hypothesis. In addition, my analysis of *Patched1* expression showed a statistically significant decrease in *Patched1* RNA expression between the wild type and mutant cell lines, which is also consistent with my hypothesis (Figure 11).

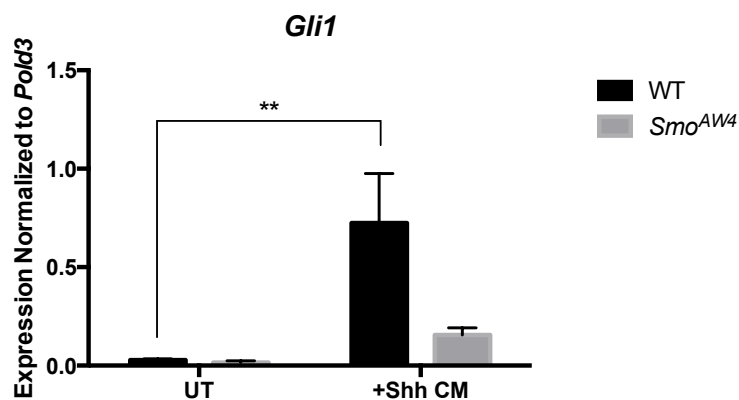


Figure 10: Transcriptional response to Shh stimulation in *Smo^{AW4}* MEFs as measured by qPCR for *Gli1*. **, significant difference ($p < 0.005$) between two conditions. (UT = 0.5% FBS / untreated; +Shh CM = treated with Shh conditioned media)

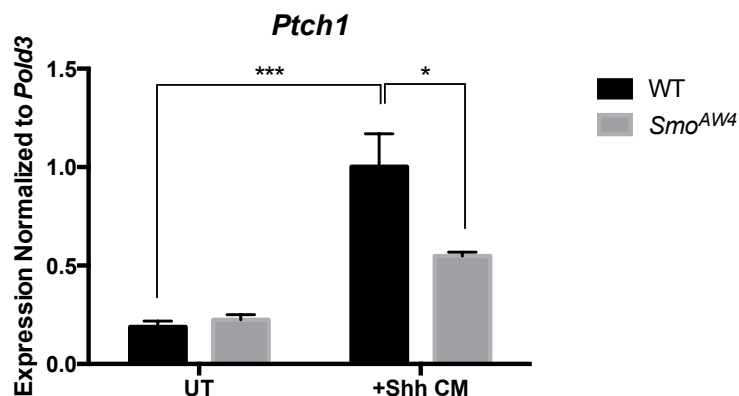


Figure 11: Transcriptional response to Shh stimulation in *Smo^{AW4}* MEFs as measured by qPCR for *Ptch1*. *, significant ($p < 0.0125$) difference between two conditions. ***, significant ($p < 0.0005$) difference between two conditions

Coverslip Immunofluorescent Staining:

I used immunofluorescent staining of coverslips to determine whether or not ciliary growth is affected by the *Smo^{AW4}* mutation and whether or not Smo is enriched in cilia after Shh treatment. MEFs on coverslips were stained with acetylated alpha-tubulin, a component of cilia. I found that the percentage of cells with cilia was similar between the WT and *Smo^{AW4}* mutants (Figure 14). Preliminary data also suggests that Smo is not enriched in cilia when cells are treated with Shh conditioned media (Figure 13). This is contrary to the wild type, which illustrates the expected enrichment based on prior knowledge of vertebrate Shh signaling (Figure 12).

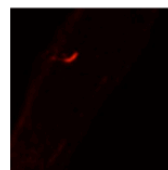
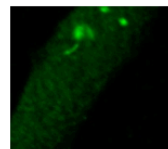
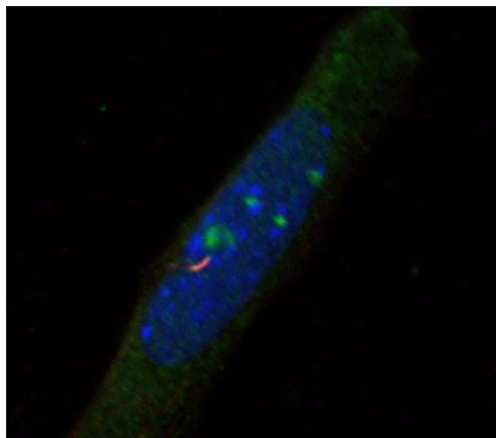


Figure 12: Wild type Shh treated cell stained for acetylated alpha-tubulin (Red) and Smoothened (Green). Illustrates expected enrichment of Smo into cilium as a result of Shh treatment.

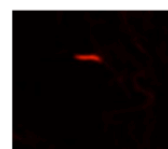
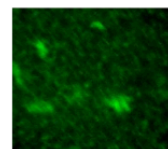
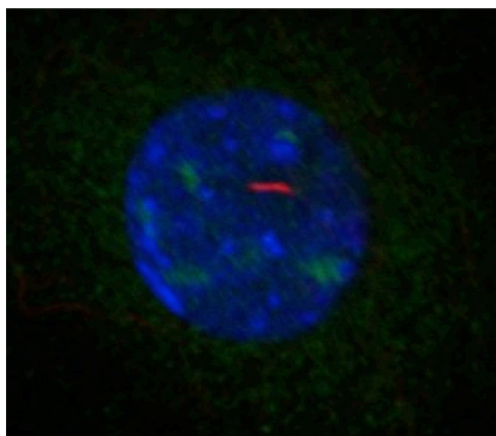


Figure 13: *Smo^{AW4}* Shh treated cell stained for acetylated alpha-tubulin (Red) and Smoothened (Green). Illustrates that Smo is not enriched in the cilium in response to Shh treatment.

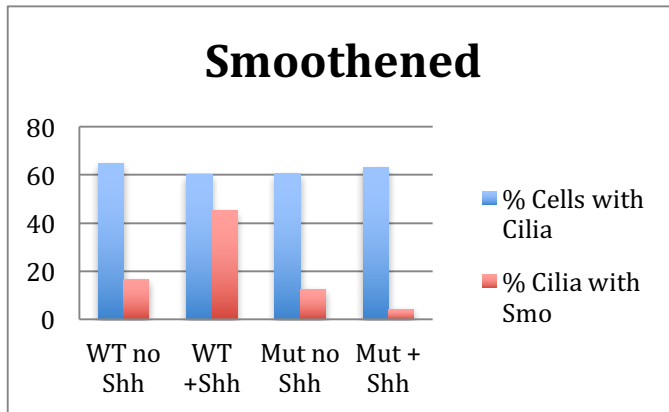


Figure 14: Percentage of MEFs with cilia (based on tubulin staining) and percentage of cilia with Smo (based on Smo staining)

Quantitative RT-PCR After SAG Treatment:

I used quantitative RT-PCR of SAG treated MEFs to measure the presence of Shh transcriptional targets, *Gli1* and *Patched1*. My preliminary data shows that *Gli1* and *Patched1* transcripts are not increased when treated with SAG in the *Smo^{AW4}* mutant cells, whereas they are up regulated by SAG in the wild type MEFs (Figures 15 and 16).

Biological replicates are necessary to validate these results.

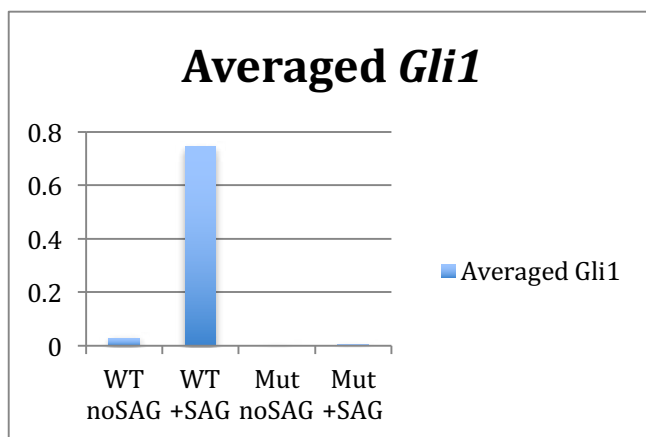


Figure 15: Transcriptional response to SAG stimulation in *Smo^{AW4}* MEFs as measured by qPCR for *Gli1*.

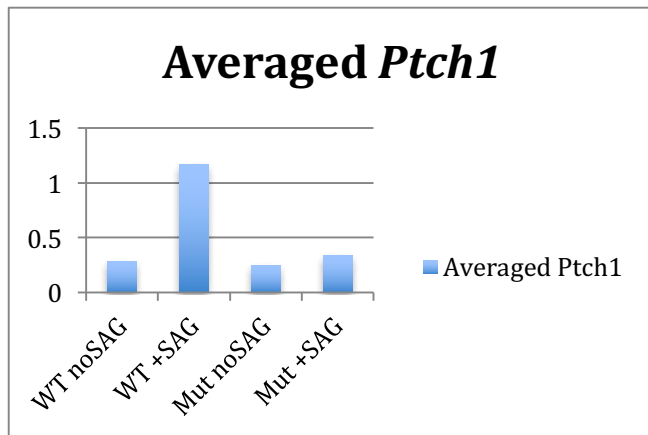


Figure 16: Transcriptional response to SAG stimulation in *Smo^{AW4}* MEFs as measured by qPCR for *Patched1*.

Discussion:

An ENU induced forward genetic screen completed in Dr. Caspary's lab prior to my involvement yielded the *Smo^{AW4}* allele. The physical phenotype presents as more vertical and medial nasal pits, shorter limbs and digits, and a rough neural tube. These characteristics are consistent with the Shh signaling pathway's involvement in nervous system, craniofacial and limb development. Genetic mapping and deep resequencing revealed that the mutation is at residue 223 of Smoothened, closer to the N-terminus of the protein just prior to the first transmembrane domain. The amino acid change is an asparagine to lysine, meaning that the residue acquires a positive charge. This new basic characteristic is consistent with a change in protein shape and potential loss of function, supporting the hypothesis that *Smo^{AW4}* is a hypomorphic allele. Smoothened is a G-protein coupled receptor that is the obligate transducer of the Sonic Hedgehog signaling pathway. Insight into this pathway can provide information on the human health disorders associated with both overactivation and underactivation of the pathway.

I examined neural tube development by looking at the proteins Shh, FoxA2, Nkx2.2, Olig2 and HB9 in order to analyze the impact of the *Smo^{AW4}* mutation on Shh signaling and its role in neural patterning. The results illustrate that signaling is occurring, although at a reduced level. The expected cell types were all present, which would not be possible without transduction of the Sonic Hedgehog signaling pathway. The domains of the various cells were smaller and shifted toward the ventral midline, consistent with reduced pathway activity. These results support the hypothesis that *Smo^{AW4}* is a hypomorphic allele.

The qPCR experiment also indicates that the *Smo^{AW4}* mutation results in decreased response to Sonic Hedgehog signaling. I found a subtle change in the neural tube patterning of the *Smo^{AW4}* mutant embryos, but saw a greater difference between wild type and mutant in the *in vitro* analysis. The statistically significant difference seen in the level of *Patched1* transcript is interesting because it would be expected that the role of *Patched1* in negative feedback would make its difference less pronounced than *Gli1*. One possible explanation for this difference is that the *Gli1* results were simply too variable to allow for statistical significance. This is supported by its p-value of .0134, which is strongly trending towards the Bonferroni corrected p-value of .0125. This could be due to the nature of *in vitro* analyses; they are artificial, individual biological runs at finite time points.

I used coverslip immunofluorescence staining to look at cilia and the localization of Smo in both wild type and mutants. In this preliminary study, I found that the percentage of ciliated cells is not affected by the *Smo^{AW4}* mutation. Interestingly, Smo is not enriched in the cilia in the *Smo^{AW4}* mutant cells after Shh stimulation, which, as described in the introduction, is believed to be necessary for Sonic hedgehog signal transduction in vertebrates. This lack of enrichment could be due to the antibody's inability to bind the

mutated protein, but I believe that this is unlikely because the antibodies used are polyclonal, thus the disruption of one site should not eradicate antibody recognition completely. Alternatively, it could mean that Smo does not need to be enriched in cilia for pathway activation. The inability to enrich in the cilia could explain the disrupted but still activated signal transduction in *Smo^{AW4}* mutants. In order to explore this further, I have created a GFP tagged construct that I will transfect into cells; then I can examine the localization of the GFP tag by immunofluorescence.

Smoothened agonist (SAG) causes constitutive Shh activation in wild type cells. SAG activates the pathway at the level of Smo (17). Quantitative RT-PCR revealed that SAG is not effective in constitutively activating the pathway in the *Smo^{AW4}* mutants. This means that the deficits in Shh signaling cannot be rescued by SAG (18). One possibility is that the *Smo^{AW4}* mutation alters the helical binding pocket where SAG interacts with Smo. An alternative possibility depends on the hypothesis that an unknown ligand is responsible for Smo activation. Perhaps this ligand binds in the same location as SAG and is thus also affected by *Smo^{AW4}*. My results thus far are based on preliminary evidence, and need to be repeated. As an additional follow up experiment, I will be analyzing coverslips of MEFs treated with SAG to see if Smo is enriched in the cilia upon treatment.

Smoothened is used as a drug target by multiple pharmaceutical companies due to the importance of Smo in Shh signaling, since overactivation of Smo and the Shh pathway causes tumors and inhibited Smo can reduce proliferation. Some cancer treatments target the binding pocket where *Smo^{AW4}* resides (Figure 17)(18). I intend to test whether the *Smo^{AW4}* mutation also affects the binding of a cancer therapy drug, LY2940680 (18).

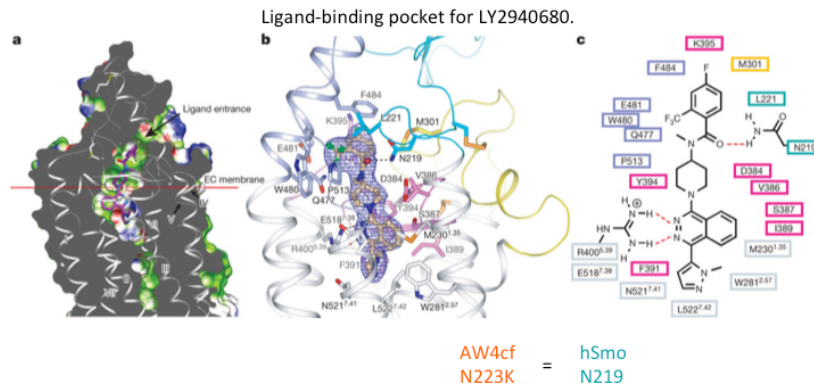


Figure 17: Binding pocket for antitumor agent LY2940680, in human Smoothed (hSmo). Human residue 219 is homologous to mouse residue 223, which is mutant in *Smo^{AW4}*. Reprinted by permission from Macmillan Publishers Ltd: Nature (18), copyright 2013

The use of mutants to learn more about signaling pathways is not new to Shh signaling (12). The finding that a point mutation in mouse Smo can cause reduced but present Shh signaling supports the formal possibility that *Smo^{AW4}* is a loss of function allele (14). My analyses of neural tube patterning, ciliary localization of Smo, overall phenotype of mutant embryos, and Shh pathway transcriptional output are all consistent with the hypothesis that *Smo^{AW4}* is a hypomorphic allele.

References:

1. Briscoe J, Therond PP. The mechanisms of Hedgehog signalling and its roles in development and disease. *Nature reviews Molecular cell biology*. 2013;14(7):416-29. Epub 2013/05/31. doi: 10.1038/nrm3598. PubMed PMID: 23719536.
2. Chiang C, Litingtung Y, Lee E, Young KE, Corden JL, Westphal H, et al. Cyclopia and defective axial patterning in mice lacking Sonic hedgehog gene function. *Nature*. 1996;383(6599):407-13. Epub 1996/10/03. doi: 10.1038/383407a0. PubMed PMID: 8837770.
3. Marigo V, Davey RA, Zuo Y, Cunningham JM, Tabin CJ. Biochemical evidence that patched is the Hedgehog receptor. *Nature*. 1996;384(6605):176-9. Epub 1996/11/14. doi: 10.1038/384176a0. PubMed PMID: 8906794.
4. Zhao Y, Tong C, Jiang J. Hedgehog regulates smoothed activity by inducing a conformational switch. *Nature*. 2007;450(7167):252-8. Epub 2007/10/26. doi: 10.1038/nature06225. PubMed PMID: 17960137.
5. Echelard Y, Epstein DJ, St-Jacques B, Shen L, Mohler J, McMahon JA, et al. Sonic hedgehog, a member of a family of putative signaling molecules, is implicated in the regulation of CNS polarity. *Cell*. 1993;75(7):1417-30. Epub 1993/12/31. PubMed PMID: 7916661.
6. Krauss S, Concordet JP, Ingham PW. A functionally conserved homolog of the *Drosophila* segment polarity gene *hh* is expressed in tissues with polarizing activity in zebrafish embryos. *Cell*. 1993;75(7):1431-44. Epub 1993/12/31. PubMed PMID: 8269519.
7. Riddle RD, Johnson RL, Laufer E, Tabin C. Sonic hedgehog mediates the polarizing activity of the ZPA. *Cell*. 1993;75(7):1401-16. Epub 1993/12/31. PubMed PMID: 8269518.
8. Corbit KC, Aanstad P, Singla V, Norman AR, Stainier DY, Reiter JF. Vertebrate Smoothed functions at the primary cilium. *Nature*. 2005;437(7061):1018-21. Epub 2005/09/02. doi: 10.1038/nature04117. PubMed PMID: 16136078.
9. Briscoe J, Ericson J. Specification of neuronal fates in the ventral neural tube. *Current opinion in neurobiology*. 2001;11(1):43-9. Epub 2001/02/17. PubMed PMID: 11179871.
10. Briscoe J, Pierani A, Jessell TM, Ericson J. A homeodomain protein code specifies progenitor cell identity and neuronal fate in the ventral neural tube. *Cell*. 2000;101(4):435-45. Epub 2000/06/01. PubMed PMID: 10830170.
11. Ericson J, Briscoe J, Rashbass P, van Heyningen V, Jessell TM. Graded sonic hedgehog signaling and the specification of cell fate in the ventral neural tube. *Cold Spring Harbor symposia on quantitative biology*. 1997;62:451-66. Epub 1997/01/01. PubMed PMID: 9598380.
12. Caspary T, Garcia-Garcia MJ, Huangfu D, Eggenschwiler JT, Wyler MR, Rakeman AS, et al. Mouse Dispatched homolog1 is required for long-range, but not juxtacrine, Hh signaling. *Current biology : CB*. 2002;12(18):1628-32. Epub 2002/10/10. PubMed PMID: 12372258.
13. Zhang XM, Ramalho-Santos M, McMahon AP. Smoothed mutants reveal redundant roles for Shh and Ihh signaling including regulation of L/R symmetry by the mouse node. *Cell*. 2001;106(2):781-92. Epub 2001/08/24. PubMed PMID: 11517919.
14. Sun M, Mondal K, Patel V, Horner VL, Long AB, Cutler DJ, et al. Multiplex Chromosomal Exome Sequencing Accelerates Identification of ENU-Induced Mutations in

- the Mouse. *G3 (Bethesda)*. 2012;2(1):143-50. Epub 2012/03/03. doi: 10.1534/g3.111.001669. PubMed PMID: 22384391; PubMed Central PMCID: PMC3276189.
15. Hynes M, Ye W, Wang K, Stone D, Murone M, Sauvage F, et al. The seven-transmembrane receptor smoothed cell-autonomously induces multiple ventral cell types. *Nature neuroscience*. 2000;3(1):41-6. Epub 1999/12/22. doi: 10.1038/71114. PubMed PMID: 10607393.
16. Caspary T, Larkins CE, Anderson KV. The graded response to Sonic Hedgehog depends on cilia architecture. *Developmental cell*. 2007;12(5):767-78. Epub 2007/05/10. doi: 10.1016/j.devcel.2007.03.004. PubMed PMID: 17488627.
17. Chen JK, Taipale J, Young KE, Maiti T, Beachy PA. Small molecule modulation of Smoothed activity. *Proceedings of the National Academy of Sciences of the United States of America*. 2002;99(22):14071-6. Epub 2002/10/23. doi: 10.1073/pnas.182542899. PubMed PMID: 12391318; PubMed Central PMCID: PMC137838.
18. Wang C, Wu H, Katritch V, Han GW, Huang XP, Liu W, et al. Structure of the human smoothed receptor bound to an antitumour agent. *Nature*. 2013;497(7449):338-43. Epub 2013/05/03. doi: 10.1038/nature12167. PubMed PMID: 23636324; PubMed Central PMCID: PMC3657389.